

High-Field ^{13}C Dynamic Nuclear Polarization with a Radical Mixture

Vladimir K. Michaelis,^{†,‡,§} Albert A. Smith,^{†,‡,§} Björn Corzilius,^{†,‡} Olesya Haze,[‡] Timothy M. Swager,[‡] and Robert G. Griffin^{*,†,‡}

[†]Francis Bitter Magnet Laboratory and [‡]Department of Chemistry, Massachusetts Institute of Technology, Cambridge, Massachusetts 02139, United States

S Supporting Information

ABSTRACT: We report direct ^{13}C dynamic nuclear polarization at 5 T under magic-angle spinning (MAS) at 82 K using a mixture of monoradicals with narrow EPR linewidths. We show the importance of optimizing both EPR linewidth and electron relaxation times by studying direct DNP of ^{13}C using SA-BDPA and trityl radical, and achieve ^{13}C enhancements above 600. This new approach may be best suited for dissolution DNP and for studies of ^1H depleted biological and other nonprotonated solids.

Over the past few decades, many techniques for studying chemical structure have been developed. NMR spectroscopy in particular has achieved widespread use because of its ability to characterize biological molecules in terms of chemical structure, dynamics, and medium-range (4–6 Å) intra- and intermolecular structure. Solid-state NMR spectroscopy (ssNMR) in particular has been especially important in structurally characterizing disordered biological solids, which are inaccessible to traditional diffraction-based methods. However, the success of these experiments is limited because of the low Boltzmann polarization of nuclear spins, leading to long acquisition times. To address this issue, solution NMR spectroscopy and magnetic resonance imaging focus primarily on high- γ , abundant nuclei such as ^1H , ^{19}F , and ^{31}P , while ssNMR methods utilize magic-angle spinning (MAS), cross-polarization (CP), and high magnetic fields to obtain modest gains in sensitivity and resolution.

More recently, high-field dynamic nuclear polarization (DNP) has been a valuable approach for studying structure, function, and reaction pathways because it allows significant reductions in acquisition times. In a DNP experiment, the large thermal electron spin polarization of a paramagnetic compound is transferred to surrounding nuclei, a process that is driven by irradiating the sample with microwaves.^{1,2} Immense gains in sensitivity have been reported for various low- γ nuclei (e.g., ^{13}C , ^{15}N , ^{17}O , ^{27}Al , and ^{29}Si) using indirect DNP polarization.^{3–6} Typically, a nitroxide-based biradical (e.g., TOTAPOL) is used as the electron polarization source and polarizes ^1H , theoretically reaching an enhancement factor (ϵ) of $\gamma_e/\gamma_H \approx 660$.^{7,8} This polarization is then transferred from ^1H to lower- γ nuclei by a CP step, reaching ϵ values as high as 248.⁹ This approach has been used successfully for structural biology and more recently surface science studies.^{4,10–18}

Indirect polarization is extremely attractive, as many systems contain ^1H nuclei that are easily polarized. Strong ^1H – ^1H and

e^- – ^1H couplings allow for efficient DNP and dispersion of polarization via spin diffusion. Additionally, the wide availability of nitroxide-based biradicals with broad EPR lines allows high- γ nuclei such as ^1H to be efficiently polarized by the cross-effect (CE). Unfortunately, many chemical systems do not fall into this category because they are severely lacking in ^1H nuclei, which limits the ability for efficient CP. An attractive approach in these circumstances is to perform direct polarization (DP) of low- γ nuclei such as ^{13}C without the CP step from ^1H .

In this work, we utilized as the polarizing agent a mixture of two narrow-line-width radicals whose EPR resonance frequencies are separated by approximately the ^{13}C nuclear Larmor frequency. Concurrently, since they exhibit different relaxation rates, we can optimize both the CE matching condition and the DNP kinetics. With this mixture, we obtained record ^{13}C DNP enhancements of >600 (nearly 25% of the theoretical enhancement, $\gamma_e/\gamma_C \approx 2620$).

The development of high-field DNP has focused on the CE mechanism, since typical solid effect (SE) enhancements are considerably lower than those for CE.¹⁹ However, recent results have shown that SE may be useful for polarization using transition-metal-based polarizing agents²⁰ and can also give enhancements of ~ 100 ;^{21,22} with sufficient microwave field strength, the sensitivity gains may match those of CE.²³ The dominant polarization transfer process depends on the nucleus being polarized and the EPR characteristics of the polarizing agent. In particular, the relative magnitudes of the electron homogeneous (δ) and inhomogeneous (Δ) linewidths and the nuclear Larmor frequency (ω_{0I}) determine the dominant polarization mechanism.

The SE mechanism is a two-spin process that is dominant when ω_{0I} is greater than δ and Δ and microwave irradiation is applied at the electron–nuclear zero- or double-quantum frequency.^{24–26} This matching condition is given by

$$\omega_{\text{mw}} = \omega_{0S} \pm \omega_{0I} \quad (1)$$

where ω_{0S} is the electron Larmor frequency and ω_{mw} is the microwave frequency.

The CE mechanism may be described as a three-spin “flip–flop–flip” process involving two electrons and a nucleus, and it is dominant when $\Delta > \omega_{0I} > \delta$. To achieve maximum efficiency, the difference between the Larmor frequencies of the two electrons must be near the nuclear Larmor frequency.^{27–31}

$$\omega_{0I} = \omega_{0S_2} - \omega_{0S_1} \quad (2)$$

Received: December 16, 2012

Published: February 4, 2013

Optimizing the polarizing agents used for SE and CE is a nontrivial task, as discussed recently by Hu.³² Both the EPR line shape and the electron spin–lattice relaxation time (T_{1S}) must be considered. For SE, one applies microwave irradiation at the matching condition given in eq 1; ideally, one uses a polarizing agent with a narrow EPR spectrum, thus allowing the matching condition to be met for the majority of the unpaired electrons in the system. Also, a short electron T_{1S} allows quick “recycling” of SE, since the electron must quickly recover its polarization in order to polarize many nuclei. However, there is an optimum value of T_{1S} , since a short T_{1S} leads to paramagnetic relaxation of nearby nuclei, thus destroying the polarization already transferred to these nuclei.

For CE, one destroys the thermal polarization of one electron with microwave irradiation. This electron then recovers its polarization via a flip–flop–flip process with a second electron and a nucleus. This process is efficient when eq 2 is satisfied. Therefore, the ideal polarizing agent includes two different radicals having narrow EPR resonances that are separated by the nuclear Larmor frequency. The recovery of the polarization of the first electron occurs via two competing processes, namely, the CE mechanism just described and the usual electron T_{1S} relaxation. Therefore, if T_{1S} of the first electron is long, the CE mechanism dominates and polarization transfer is more efficient, as recently demonstrated by Zagdoun et al.⁸ This is not a complete picture, however. The second electron must provide polarization, as does the electron in SE. Therefore, quick recycling of the CE mechanism relies on a sufficiently short T_{1S} of the second electron. If the two electrons have the same T_{1S} , as is the case for most nitroxide biradicals, then one must compromise on T_{1S} . However, if two different radicals are used, then one can select polarizing agents in which the first electron has a long T_{1S} and the second electron has a shorter T_{1S} .

We have demonstrated efficient CE by using a mixture of two organic water-soluble polarizing agents, SA-BDPA³³ and the trityl radical OX063³⁴ (Figure 1), which have relatively narrow

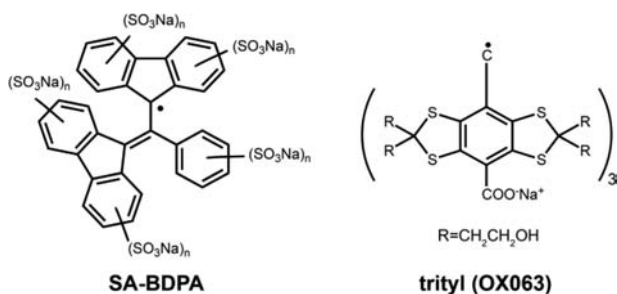


Figure 1. Chemical structures of the narrow-line monoradicals SA-BDPA and trityl (OX063).

EPR linewidths of 28 and 50 MHz, respectively. The centers of the EPR spectra are separated by roughly the ^{13}C Larmor frequency (34 MHz separation vs 53 MHz Larmor frequency at 5 T; the linewidth of trityl is broad enough to make up the difference). Additionally, SA-BDPA has a long T_{1S} , whereas the T_{1S} of trityl is shorter,³³ giving improved CE performance when irradiating near the SA-BDPA resonance.

^{13}C DP MAS NMR experiments were performed using SA-BDPA and OX063 (hereafter denoted as “trityl”). Both SE and CE had to be considered in this study. To evaluate the dominant DNP mechanism, the ^{13}C DNP enhancement field

profiles were measured via direct detection, where the magnetic field was adjusted to between 4977 and 4990 mT and a microwave output power of 8 W was chosen for long-term stability (>6 h).

Figure 2A shows EPR spectra of SA-BDPA and trityl acquired at 140 GHz (the field axis was adjusted to align with

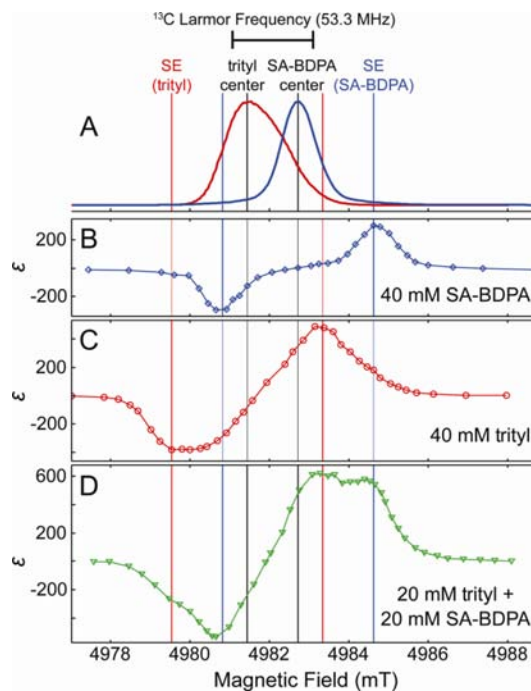


Figure 2. (A) EPR spectra of SA-BDPA and trityl and (B–D) field-dependent ^{13}C DNP enhancement profiles of (B) SA-BDPA, (C) trityl, and (D) a 1:1 mixture. The field profiles were recorded at 82 K with a microwave frequency of 139.66 GHz, a microwave power of 8 W, and a MAS frequency of 4.8 kHz.

the DNP experiments at 139.66 GHz). The center of each spectrum is marked in black, and the field positions predicted to be optimal for SE DNP of SA-BDPA and trityl are marked in blue and red, respectively. Figure 2B–D shows ^{13}C DNP field profiles for SA-BDPA, trityl, and a 1:1 mixture, each with a total radical concentration of 40 mM.

Figure 2B shows the field profile using only SA-BDPA. The EPR spectrum shows that the SA-BDPA resonance is narrower than the ^{13}C Larmor frequency. Therefore, SE should strongly dominate the DNP transfer. This was confirmed by the plateau in the enhancement at the center of the DNP field profile, which is characteristic of well-resolved SE. Also the position of maximum enhancement is in good agreement with the position predicted for SE.

The trityl EPR spectrum is considerably broader than that of SA-BDPA, and with the linewidth of 50 MHz it should be possible for both SE and CE to contribute to the DNP enhancement. The trityl DNP profile is given in Figure 2C. The asymmetry of the enhancements (−380 vs 480) and the lack of a plateau in the center of the field profile suggest that CE makes some contribution to the DNP enhancement. However, the extrema of the DNP profile are in good agreement with those predicted for SE DNP, indicating that SE also likely makes a major contribution.

Figure 2D shows the ^{13}C DNP field profile for a 1:1 mixture of SA-BDPA and trityl. In this case, there are many contributing

DNP processes: SE resulting from SA-BDPA, SE and CE resulting from trityl, and finally CE resulting from the interaction between SA-BDPA and trityl. Careful examination revealed that the major features in the field profile are at nearly the same positions as seen in the profiles of pure SA-BDPA and trityl. We first examine the features seen at 4980.7 and 4984.4 mT, which correspond to SE from SA-BDPA. The intensity of these features is remarkable, giving enhancements of -535 and 575 , respectively. Although other processes contribute to these large enhancements, it appears that SE from SA-BDPA is at least as effective in this sample as it was in the pure SA-BDPA sample, despite the total concentration of SA-BDPA in the mixed sample being half of that in the pure sample. This was further confirmed by subtracting the SA-BDPA DNP field profile from the mixture field profile using a coefficient of 1.1, which was chosen to remove the features resulting from SE using SA-BDPA fully without introducing other features (Figure 3). This implies that SE resulting from

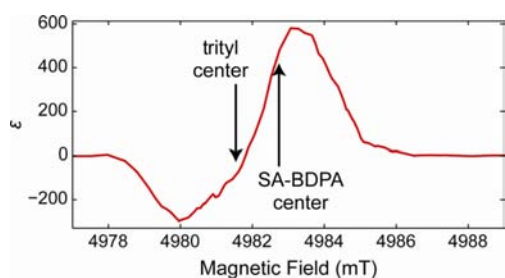


Figure 3. DNP field profile obtained by subtracting the SA-BDPA DNP field profile in Figure 2B (multiplied by 1.1) from the DNP field profile for the SA-BDPA/trityl mixture.

SA-BDPA is somehow more effective in this sample than in the pure sample. In fact, this is a result of a reduced electron T_{1S} for SA-BDPA in the mixed sample. Paramagnetic relaxation from trityl actually shortened the SA-BDPA T_{1S} from 28.9 ms in the pure SA-BDPA sample to 3.6 ms in the mixture (Table 1), allowing SA-BDPA to become more efficient at polarizing the ^{13}C nuclei. We also note that the change in the trityl T_{1S} was negligible.

Table 1. ^{13}C Direct Detection Enhancements (ϵ), Electron Spin Relaxation Times (T_{1S}), and DNP Buildup Times (T_B)

radical	ϵ	T_{1S} (ms)	T_B (s)
SA-BDPA (40 mM)	300	28.9	287 (16)
trityl (40 mM)	480	1.4	167 (7)
1:1 mixture (each 20 mM)	620	3.6 (SA-BDPA) 1.4 (trityl)	216 (3)

After removal of the SA-BDPA SE contribution, a highly asymmetric DNP field profile remains (Figure 3). This profile contains contributions from pure-trityl SE and CE as well as CE resulting from SA-BDPA and trityl. The pure-trityl field profile (Figure 2C) is not nearly as asymmetric as this profile, so this asymmetry is likely a result of CE from SA-BDPA and trityl. In fact, this is exactly what we would expect. If we irradiate near the center of the SA-BDPA spectrum, the SA-BDPA radical should saturate easily, since it has a longer T_{1S} . Therefore, the polarization recovery of the SA-BDPA electron should occur primarily via the CE mechanism. Furthermore, the short T_{1S} of trityl should allow for quick recycling of the CE mechanism,

giving an overall more efficient CE mechanism. However, irradiation closer to the center of the trityl spectrum should make saturation more difficult because the T_{1S} of trityl is shorter and the source of polarization, SA-BDPA, recovers more slowly. This should lead to an overall less efficient CE mechanism. We note that the peaks do not lie exactly on the SA-BDPA and trityl centers. This occurs both because SA-BDPA and trityl do not have exactly the correct separation for the ^{13}C CE matching and because contributions to the DNP enhancement from the pure trityl remain. One should note that previous experiments by Hu et al.¹⁹ showed that mixtures of TEMPO and trityl are efficient in polarizing ^1H . In particular, the DNP was efficient when the narrow trityl radical line was irradiated. However, it was not clear whether the improvements were primarily due to a longer electron T_1 for trityl or the considerably narrower line shape of trityl compared with TEMPO.

Both the nuclear spin–lattice relaxation times (T_{1I}) and the polarization buildup times (T_B) for ^{13}C were measured at 82 K. The T_B and T_{1I} values were within the error of one another for each radical composition, so only T_B is listed in Table 1. T_B varied between the radicals, however, with trityl having the shortest T_B and SA-BDPA the longest. The radical concentrations and sample conditions were identical, enabling direct comparison of the effects of the nuclear and electron relaxation characteristics. The observed reduction in polarization times for each sample must be attributed to the inherent electron T_{1S} of the radical and the type of DNP mechanisms that are active.

Direct ^{13}C polarization enhancements were measured at the maximum positive field positions using optimized recycle delays ($1.26T_B$) for each radical composition (Figure 4). Off signals

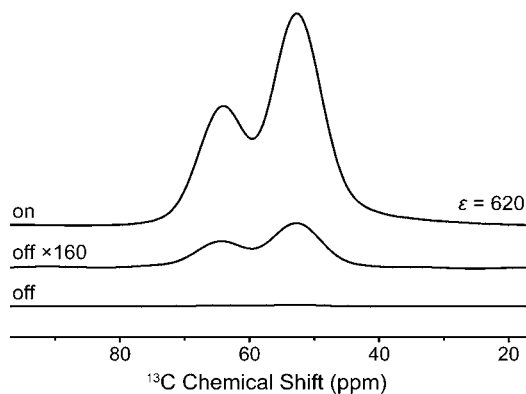


Figure 4. Direct ^{13}C polarization using the SA-BDPA (20 mM)/trityl (20 mM) mixture in 6:3:1 [$U\text{-}^{13}\text{C}$]glycerol- d_8 /D $_2$ O/H $_2$ O at 82 K and 10 W ($B_0 = 4983.1$ mT).

(microwave power of 0 W) were acquired under conditions identical to those for the on signals (microwave power of 10 W) for SA-BDPA (4984.5 mT), trityl (4983.2 mT), and the mixture (4983.1 mT). SA-BDPA and trityl provided enhancements of 300 and 480, respectively, at 82 K. The result for SA-BDPA is comparable to that of previous studies on ^{13}C detection using TOTAPOL, where enhancements of 305 were obtained under similar sample conditions.³⁵ Trityl proved to be slightly more efficient at polarization, providing $\sim 60\%$ larger enhancement, as the breadth better satisfies the CE mechanism. The mixed-radical sample satisfied the CE matching condition most efficiently, and the beneficial differences in T_{1S} led to a very effective CE enhancement of 620. The mixture out-

performed trityl (>130%) and SA-BDPA (>200%) as well as previous experiments that utilized TOTAPOL for ^{13}C DNP (>200%).³⁵

These narrow-line radicals may be ideally suited for DP of low- γ nuclei that are either poorly cross-polarized by high- γ nuclei (e.g., ^1H or ^{19}F) or are found within environments in which high- γ nuclei are absent. Using a mixture of radicals that satisfy the CE matching condition better and have different T_{1S} relaxation times could have drastic implications, providing a more efficient CE mechanism and helping to compensate for the decrease in enhancement as DNP experiments move to higher magnetic fields. These findings may be beneficial for dissolution DNP methods that commonly use trityl radical, since one may combine SA-BDPA and trityl. Then, polarizing at liquid He temperatures could lead to significant polarization gains in labeled dissolution experiments without modification of any hardware. Finally, if trityl and SA-BDPA can be tethered together to create a biradical, it should be possible to reduce the radical concentrations, increase the contribution of CE to the DNP enhancements, and potentially increase DNP gains in the future.

■ ASSOCIATED CONTENT

● Supporting Information

Experimental methods and sample preparation. This material is available free of charge via the Internet at <http://pubs.acs.org>.

■ AUTHOR INFORMATION

Corresponding Author

rgg@mit.edu

Author Contributions

[§]V.K.M. and A.A.S. contributed equally.

Notes

The authors declare no competing financial interest.

■ ACKNOWLEDGMENTS

The research reported in this publication was supported by the National Institute of Biomedical Imaging and Bioengineering of the National Institutes of Health under Awards EB-002804, EB-002026, EB-001960, and GM-095843. V.K.M. is grateful to the Natural Sciences and Engineering Research Council of Canada for a postdoctoral fellowship. B.C. acknowledges a research fellowship from the Deutsche Forschungsgemeinschaft (CO 802/1-1).

■ REFERENCES

- (1) Carver, T. R.; Slichter, C. P. *Phys. Rev.* **1953**, *92*, 212.
- (2) Overhauser, A. W. *Phys. Rev.* **1953**, *92*, 411.
- (3) Becerra, L. R.; Gerfen, G. J.; Temkin, R. J.; Singel, D. J.; Griffin, R. G. *Phys. Rev. Lett.* **1993**, *71*, 3561.
- (4) Lesage, A.; Lelli, M.; Gajan, D.; Caporini, M. A.; Vitzthum, V.; Mieville, P.; Alauzun, J.; Roussey, A.; Thieuleux, C.; Mehdi, A.; Bodenhausen, G.; Coperet, C.; Emsley, L. *J. Am. Chem. Soc.* **2010**, *132*, 15459.
- (5) Michaelis, V. K.; Markhasin, E.; Daviso, E.; Herzfeld, J.; Griffin, R. G. *J. Phys. Chem. Lett.* **2012**, *3*, 2030.
- (6) Vitzthum, V.; Mieville, P.; Carnevale, D.; Caporini, M. A.; Gajan, D.; Coperet, C.; Lelli, M.; Zagdoun, A.; Rossini, A. J.; Lesage, A. *Chem. Commun.* **2012**, *48*, 1988.
- (7) Song, C.; Hu, K.-N.; Joo, C.-G.; Swager, T. M.; Griffin, R. G. *J. Am. Chem. Soc.* **2006**, *128*, 11385.
- (8) Zagdoun, A.; Casano, G.; Ouari, O.; Lapadula, G.; Rossini, A. J.; Lelli, M.; Baffert, M.; Gajan, D.; Veyre, L.; Maas, W. E.; Rosay, M. M.;

Weber, R. T.; Thieuleux, C.; Coperet, C.; Lesage, A.; Tordo, P.; Emsley, L. *J. Am. Chem. Soc.* **2012**, *134*, 2284.

(9) Kieseewetter, M. K.; Corzilius, B.; Smith, A. A.; Griffin, R. G.; Swager, T. M. *J. Am. Chem. Soc.* **2012**, *134*, 4537.

(10) Lelli, M.; Gajan, D.; Lesage, A.; Caporini, M. A.; Vitzthum, V.; Mieville, P.; Heroguel, F.; Rascon, F.; Roussey, A.; Thieuleux, C.; Boualleg, M.; Veyre, L.; Bodenhausen, G.; Coperet, C.; Emsley, L. *J. Am. Chem. Soc.* **2011**, *133*, 2104.

(11) Debelouchina, G. T.; Bayro, M. J.; van der Wel, P. C. A.; Caporini, M. A.; Barnes, A. B.; Rosay, M.; Maas, W. E.; Griffin, R. G. *Phys. Chem. Chem. Phys.* **2010**, *12*, 5911.

(12) Bajaj, V. S.; Mak-Jurkauskas, M. L.; Belenky, M.; Herzfeld, J.; Griffin, R. G. *Proc. Natl. Acad. Sci. U.S.A.* **2009**, *106*, 9244.

(13) Hall, D. A.; Maus, D. C.; Gerfen, G. J.; Inati, S. J.; Becerra, L. R.; Dahlquist, F. W.; Griffin, R. G. *Science* **1997**, *276*, 930.

(14) van der Wel, P. C. A.; Hu, K.-N.; Lewandowski, J.; Griffin, R. G. *J. Am. Chem. Soc.* **2006**, *128*, 10840.

(15) Bayro, M. J.; Debelouchina, G. T.; Eddy, M. T.; Birkett, N. R.; MacPhee, C. E.; Rosay, M.; Maas, W. E.; Dobson, C. M.; Griffin, R. G. *J. Am. Chem. Soc.* **2011**, *133*, 13967.

(16) Sergeev, I. V.; Day, L. A.; Goldbourt, A.; McDermott, A. E. *J. Am. Chem. Soc.* **2011**, *133*, 20208.

(17) Akbey, Ü.; Franks, W. T.; Linden, A.; Lange, S.; Griffin, R. G.; van Rossum, B.-J.; Oschkinat, H. *Angew. Chem., Int. Ed.* **2010**, *49*, 7803.

(18) Renault, M.; Pawsey, S.; Bos, M. P.; Koers, E. J.; Nand, D.; Tommassen-van Boxel, R.; Rosay, M.; Tommassen, J.; Maas, W. E.; Baldus, M. *Angew. Chem., Int. Ed.* **2012**, *51*, 2998.

(19) Hu, K.; Bajaj, V.; Rosay, M.; Griffin, R. *J. Chem. Phys.* **2007**, *126*, No. 044512.

(20) Corzilius, B.; Smith, A. A.; Barnes, A. B.; Luchinat, C.; Bertini, I.; Griffin, R. G. *J. Am. Chem. Soc.* **2011**, *133*, 5648.

(21) Smith, A. A.; Corzilius, B.; Barnes, A. B.; Maly, T.; Griffin, R. G. *J. Chem. Phys.* **2012**, *136*, No. 015101.

(22) Corzilius, B.; Smith, A. A.; Griffin, R. G. *J. Chem. Phys.* **2012**, *137*, No. 054201.

(23) Smith, A. A.; Corzilius, B.; Bryant, J. A.; DeRocher, R.; Woskov, P. P.; Temkin, R. J.; Griffin, R. G. *J. Magn. Reson.* **2012**, *223*, 170.

(24) Abragam, A.; Proctor, W. G. C. R. *Hebd. Seances Acad. Sci.* **1958**, *246*, 2253.

(25) Jeffries, C. D. *Phys. Rev.* **1960**, *117*, 1056.

(26) Hovav, Y.; Feintuch, A.; Vega, S. *J. Magn. Reson.* **2010**, *207*, 176.

(27) Kessenikh, A. V.; Lushchikov, V. I.; Manenkov, A. A.; Taran, Y. V. *Sov. Phys.—Solid State* **1963**, *5*, 321.

(28) Hwang, C. F.; Hill, D. A. *Phys. Rev. Lett.* **1967**, *18*, 110.

(29) Hu, K.-N.; Debelouchina, G. T.; Smith, A. A.; Griffin, R. G. *J. Chem. Phys.* **2011**, *134*, No. 125105.

(30) Hovav, Y.; Feintuch, A.; Vega, S. *J. Magn. Reson.* **2012**, *214*, 29.

(31) Thurber, K. R.; Tycko, R. *J. Chem. Phys.* **2012**, *137*, No. 084508.

(32) Hu, K.-N. *Solid State Nucl. Magn. Reson.* **2011**, *40*, 31.

(33) Haze, O.; Corzilius, B.; Smith, A. A.; Griffin, R. G.; Swager, T. M. *J. Am. Chem. Soc.* **2012**, *134*, 14287.

(34) Ardenkjaer-Larsen, J.; Laursen, I.; Leunbach, I.; Ehnholm, G.; Wistrand, L.; Petersson, J.; Golman, K. *J. Magn. Reson.* **1998**, *133*, 1.

(35) Maly, T.; Miller, A.-F.; Griffin, R. G. *ChemPhysChem* **2010**, *11*, 999.